Cancer Metastasis Rev (2008) 27:615–630
DOI 10.1007/s10555-008-9147-6

Non-invasive assessment of tumor neovasculature: techniques and clinical applications

Rodolfo Perini · Regine Choe · Arjun G. Yodh · Chandra Sehgal · Chaitanya R. Divgi · Mark A. Rosen

Published online: 28 May 2008

Abstract The ability to induce and sustain angiogenesis is regarded as one of the hallmarks of cancer growth and metastasis. Marked advances in understanding vascular physiology and mechanisms of angiogenesis have led to the development of vascularly-targeted anti-cancer therapies. Two broad subclasses of agents are in clinical use currently: those with anti-angiogenic activity (i.e. those that target angiogenic pathways) and those that have direct cytotoxic activity against proliferating endothelial cells (i.e. vascular disruptive agents (VDAs)). This article reviews the various imaging modalities, including magnetic resonance imaging, computed tomography, photon emission imaging (positron emission tomography and single photon emission computed tomography), ultrasound and optical (near-infrared absorption and scattering) techniques that have been used in an attempt to assess the status of tumor neovasculature *in vivo*. In each case, we describe the basic imaging methodology, methods for image quantification, technical standardization and reproducibility, and current and potential clinical applications for monitoring the status of tumor neovasculature before and during treatment with vascular targeted agents.

Keywords Magnetic resonance imaging · Perfusion CT · Positron emission tomography · Vascular physiologic parameters · Anti-angiogenic therapy

R. Perini · C. Sehgal · C. R. Divgi · M. A. Rosen (✉)
Department of Radiology,
Hospital of the University of Pennsylvania,
3400 Spruce Street,
Philadelphia, PA 19104, USA
e-mail: mark.rosen@uphs.upenn.edu

R. Perini
e-mail: rodolfo.perini@uphs.upenn.edu

C. Sehgal
e-mail: sehgalc@uphs.upenn.edu

C. R. Divgi
e-mail: chaitanya.divgi@uphs.upenn.edu

R. Choe · A. G. Yodh
Department of Physics and Astronomy,
University of Pennsylvania,
209 South 33rd St,
Philadelphia, PA 19104, USA

R. Choe
e-mail: rgchoe@sas.upenn.edu

A. G. Yodh
e-mail: yodh@physics.upenn.edu

A. G. Yodh
Department of Radiation Oncology, University of Pennsylvania,
Philadelphia, PA, USA

C. R. Divgi · M. A. Rosen
Abrahamson Cancer Center, University of Pennsylvania,
Philadelphia, PA, USA

1 Introduction

In order to maintain growth above a few millimeters in diameter, all malignant tumors require in growth of new blood vessels, a process termed angiogenesis. [1] The existence of the angiogenic signaling by malignant tumors is now established as a basic biologic mechanism of tumor progression. The molecular pathways involved in angiogenesis have been defined, and provide therapeutic avenues for disrupting these pathways. Several anti-tumor agents exploiting these pathways have now been approved for use in humans, either as single agents or in combination with conventional cytotoxic therapies [2].

With the advent of anti-vascular therapies entering the clinical domain, there is increased interest in determining the *in vivo* effectiveness (or lack thereof) of these agents

in patients. Given the novel mechanism of action of these targeted agents, the classical definition of tumor response, tumor size reduction, may need to be revised. Thus there is a need for better understanding of how imaging methods may be utilized to assess the physiologic status of the tumor neovasculature and to accurately assess the activity of these agents in clinical use. This article reviews the various imaging-based methods that have been proposed or used as a means of assessing the tumor neovasculature. These methods fall into five classes: magnetic resonance imaging (MRI) techniques (most notably Dynamic Contrast Enhanced-MRI), perfusion computed tomography (CT), nuclear medicine methods (namely positron emission tomography (PET) and single photon imaging), ultrasound (US) methods (intrinsic Doppler and contrast-based methods), and optical (near-infrared (IR)) methods. In each case, we describe the basic imaging methodology, including methods of quantifying the specific imaging-based metric(es) relating to tumor vascular status. We also review existing results in human studies utilizing these methods to probe the effect of conventional and vascular targeted agents on the tumor neovasculature.

2 Vascular physiologic parameters: definition of terms

Tumor blood volume is the ratio of tumor intravascular volume to total tumor volume. It can be estimated from imaging studies when the tracer or contrast agent used remains solely within the vascular space (e.g. radioactive labeling of red blood cells). In steady-state imaging, tumor blood volume is estimated by comparing the tumoral vs. blood pool tracer concentration. In dynamic imaging, blood volume is defined by relative wash-in and wash-out of the tracer. Tumor blood volume can also be measured indirectly through measurement of total tumor hemoglobin concentration as assessed by optical imaging.

Tumor blood flow is the volume of blood that reaches the tumor over a period of time (in milliliter per minute). *Tumor perfusion* is the amount of flow per unit weight of tissue, typically in milliliter per minute per milligram tissue. Tumor blood flow can be assessed by measuring the rate of tumor accumulation of a freely diffusible agent or using tracers with high first pass extraction.

When imaging is performed with a partially diffusible agent (e.g. small molecular weight gadolinium agent in dynamic contrast enhanced MRI (DCE-MRI)), a kinetic term, K^{trans} (in per minute), is defined, representing the first order kinetic constant of tracer passage from plasma to tumor interstitium. In tumors for whom flow is limiting (e.g. high vessel permeability), $K^{trans}$is equivalent to tumor perfusion over a unit volume (e.g. milliliter per minute per milliliter). More generally, K^{trans} represents a mixture of tumor perfusion and tumor vascular permeability**.** For contrast agents with limited volume of distribution (e.g. gadolinium or iodinated agents that do not enter into intact cells), the term v^e, representing the perfused extracellular volume fraction, is also defined.

3 Magnetic resonance imaging methods

3.1 Dynamic contrast-enhanced MRI

DCE-MRI utilizes existing small molecular-weight gadolinium-based contrast agents to interrogate the status of the tumor neovasculature. DCE-MRI is performed by imaging the tumors at high temporal resolution during the early first-pass bolus and subsequent "equilibrium" phases of contrast entry into the tumor interstitium. Thus, while the imaging techniques in DCE-MRI, namely contrast-enhanced T1-weighted imaging, essentially replicate the techniques used routinely in contrast enhanced MRI, aspects of the DCE-MRI exam differ from that of a routine MRI study. These issues have been reviewed elsewhere [3, 4], and general guidelines for minimal image requirements for DCE-MRI have been published [5, 6]. To summarize the essential aspects of a DCE-MRI examination:

- DCE-MRI requires a means to quantify the amount gadolinium entering the tumor from the image enhancement ("brightening"). This generally requires information regarding the magnetic properties of the tumor, often referred to as a tumor "T1 map".
- DCE-MRI is usually performed at higher temporal resolution than that of contrast-enhanced imaging performed routinely in clinical imaging centers. While exact requirements are debated, imaging speeds on the order of one frame per 6–8 s [7] (and sometimes as high as one frame per second [8]) are generally advocated.
- At these imaging speeds, existing MRI technology does not allow for whole body, or even whole organ imaging. Thus the DCE-MRI study requires advanced planning to determine a target lesion and preferred imaging plane/geometry before the patient is scanned.

Due to these requirements, DCE-MRI studies to date are generally performed at imaging centers with specialists experienced in DCE-MRI studies. However, a DCE-MRI study can potentially be performed at any MR imaging center with modern equipment.

The key to DCE-MRI analysis is to determine the kinetic delivery of gadolinium contrast into the tumor. This requires knowledge of the arterial and tumor gadolinium concentrations during the course of gadolinium infusion and entry into the tumors. In MRI, gadolinium is indirectly imaged based on its magnetic effect on neighboring water

molecules. Thus, the relationship between gadolinium concentration and tumor enhancement on MRI is complex, and is further complicated by the nature of the gadolinium agents. The majority of the gadolinium-contrast agents approved for clinical use are small molecular-weight chelates of gadolinium, which passively diffuse across the capillary endothelial membrane, but do not cross intact tumor or tissue cell membranes. Thus, gadolinium contrast agents distribute only into the tumor extracellular space, complicating quantification of tumor or tissue gadolinium concentration.

Nevertheless, despite these obstacles, many investigators have succeeded in obtaining qualitative and quantitative kinetic evaluations of tumor enhancement in DCE-MRI studies. Two main methods for quantitating tumor gadolinium kinetics have been proposed. Evelhoch [9] proposed the "initial-area-under-the-gadolinium-curve" (IAUGC) metric, quantitating the total gadolinium uptake over the first 60 or 90 s after the arrival of contrast to the tumor. The advantage of this method is its simplicity. However, it does not take into account inter- or intra-patient variations in bolus arrival of the gadolinium in the arterial system (such as may occur due to variations in cardiac function). Furthermore, IAUGC is an abstract metric, not related directly to any physiologic measure such as tumor perfusion. Many investigators therefore favor the general kinetic model for two compartment tracer kinetics [10], more recently reformulated for DCE-MRI [11–13]. In this model, tumor enhancement is described by two parameters, K^{trans}, the unidirectional first-order kinetic constant describing transport of gadolinium between the vascular compartment and the tumor interstitium, and v^e, the extravascular, extra-cellular volume fraction of the tumor. k^{ep}, the first-order reverse transport constant for efflux of gadolinium back into the vascular space, is then given by: K^{trans}/v^e. The metric K^{trans} generally reflects both tumor blood flow and the vascular permeability-surface area product, a measure of tumor neovascular permeability. Therefore, DCE-MRI does not strictly assess tumor blood flow or perfusion, but is rather a metric reflecting the overall rate of gadolinium delivery to the tumor, and thus is an indirect marker of the status of the tumor neovasculature. More recent approaches to DCE-MRI studies have incorporated additional terms into the kinetic modeling, including a correlation time (τ_c) relating to the kinetics of water exchange between the intra- and extra-cellular tumor compartments [14], and a finite intra-tumoral vascular volume fraction (v^p) [15]. These additional parameters can improve the modeling fit of the tumor enhancement data, but require more complex software algorithms for image quantitation.

Many questions have arisen in regards to the reproducibility of DCE-MRI tumor metrics. Given the large number of image-based inputs required for estimating tumor K^{trans}, the difficulties in standardizing MR imaging intensities, and the variety of imaging and modeling techniques in use, technical variations may overwhelm the ability of researchers to reliably depict subtle alterations in tumor vascularity. Indices of repeatability for DCE-MRI metrics have suggested that with current techniques, post treatment decrements in tumor K^{trans} on the order of 40% are required to be considered a significant indicator of anti-vascular activity [16–18].

Sources of error in DCE-MRI estimates continue to be debated, including issues relating to image acquisition technique [19], modeling of the arterial input function [20], and temporal resolution [7]. Most investigators counsel that test-retest repeatability measures pre-treatment are indicated in studies that seek to use DCE-MRI for quantifying treatment-induced changes in tumor vasculature, especially studies in which DCE-MRI is applied in a multi-site setting.

3.2 DCE-MRI uses in clinical studies

It has long been recognized that, given time, effective cytotoxic therapies will blunt tumor angiogenesis [21]. As such, K^{trans} decreases in tumors responding to conventional cytotoxic therapies may be expected over time. However, in such cases, it is uncertain whether the chemotherapy has any direct anti-vascular action. More likely, it is the direct cytotoxic effect of the chemotherapy agent(s) on tumor cells which decreases the angiogenic signal required to maintain the tumor neovascularity. However, it has been shown recently [17], that within the limits of test-retest reproducibility, no change in measured tumor K^{trans}, k^{ep}, or v^e could be identified 1 day after the first dose of taxane or platinum based conventional cytotoxic regimens. These results suggest that cytotoxic therapies, even if ultimately effective in reducing tumor size, may not manifest in alterations in tumor neovasculature in the early post-treatment setting. These findings are important to bear in mind in studies where targeted agents are used in tandem with conventional cytotoxic therapies.

A number of studies have used DCE-MRI to evaluate alterations in tumor neovasculature following treatment with anti-angiogenic agents within early phase clinical trials [22–28]. Many of these reports were in phase I studies of mixed tumor types performed on a small number of patients at single imaging centers. However, despite the limited scope of these trials, useful pharmacodynamic information was often derived with the addition of DCE-MRI. In the phase I study of PTK/ZK in liver metastases, for example, changes in tumor vascular status as assessed by DCE-MRI were used to define the minimal biologically active dose [22]. In another example, DCE-MRI was used to demonstrate a dose/response relationship in a phase I study of AG-013736

in solid tumors, again providing useful information for phase II dosing [23].

Other studies have evaluated the use of DCE-MRI to gauge the effectiveness of anti-angiogenic agents directed toward a single tumor type. Wedam and colleagues demonstrated a significant decline in DCE-MRI metrics in locally advanced breast cancer after a single dose of bevacizumab [28]. In a study of metastatic colon cancer response to PTK/ZK [27], Morgan and colleagues used DCE-MRI on day two of the first cycle, and found that decreases in tumor *Ki* (a DCE-MRI index analogous to K^{trans}) were predictive of tumor shrinkage following two cycles of chemotherapy. Furthermore, dose-response analysis via DCE-MRI was successfully used in this study to inform the phase II dose, as the maximally tolerated dose was not obtained by conventional measures of toxicity. Preliminary data from two groups [29, 30] evaluating the use of DCE-MRI in advanced renal cell carcinoma undergoing sorafenib treatment have both demonstrated marked declines in tumor K^{trans} within 4–8 weeks of therapy. However, in both studies, initial tumor K^{trans}, rather than percent K^{trans} decline, were most predictive of clinical responsiveness. These results will require further validation, as absolute K^{trans} quantification in DCE-MRI can be highly dependent on the type of imaging and modeling system used.

A smaller number of human trials using DCE-MRI to evaluate tumor response to VDAs have been reported [31–35]. The most carefully studied compound in this class is the A4 phosphate analogue of combretastin, CA4P. Three separate groups evaluated this agent by DCE-MRI in a phase I setting [32–34]. Dosing regimens differed slightly, as did DCE-MRI acquisition and analytic methods, making comparisons between the studies difficult. However, all studies demonstrated a decrease in DCE-MRI indices in some patients within 6 h of dosing (Fig. 1). In one study [33], this effect was shown to be reversible at 24 h, and a minimal biologically active dose of 52 mg/m^2 was suggested. In general, the optimal time course for evaluating immediate VDA activity against tumor neovasculature in humans has not been established, and the duration of such action has not been broadly determined. Given the need to wait for gadolinium clearance before re-testing by DCE-MRI (generally 6–8 h in patients with normal renal function) repeated tumor evaluation by this method is not generally feasible in the clinical setting.

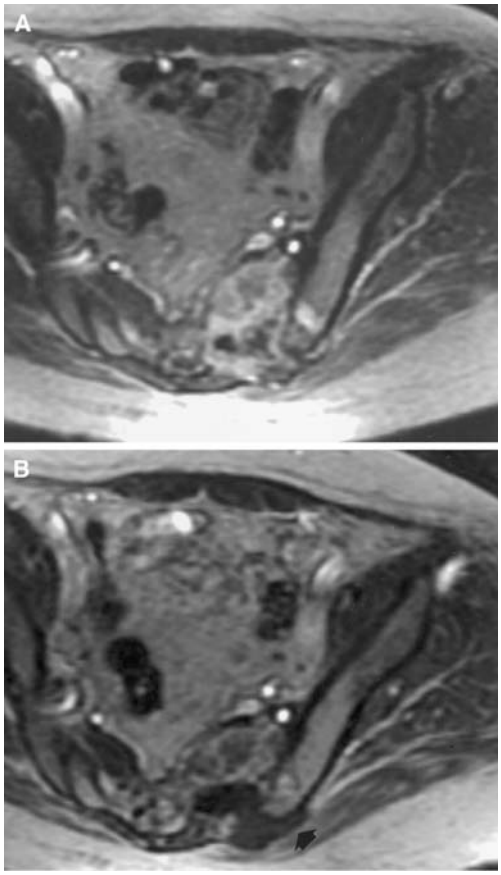

Fig. 1 Contrast-enhanced images of a sacral metastasis from a papillary thyroid tumor before (**A**) and after the day 5 dose (**B**) of CA4P. Note absent enhancement in inferior portion of the tumor after treatment (*arrow*). DCE-MRI allows for tracking of contrast delivery in tumors at high resolution, and can supply information regarding intra-lesional heterogeneity of tumor vascular response to targeted therapies (from Stevenson JP et. al. Phase I trial of the antivascular agent combretastatin A4 phosphate on a 5-day schedule to patients with cancer: magnetic resonance imaging evidence for altered tumor blood flow. J Clin Oncol. Volume 21. 2003. p 4428–38, with permission)

3.3 DCE-MRI with high molecular weight contrast agents

Most currently available clinical gadolinium agents are small gadolinium chelates with relatively low molecular weight (LMW). These agents are highly permeable, and can pass through the capillary endothelial membrane rapidly. In such cases, the measured tumor K^{trans} may reflect a combination of both tumor blood flow and neovascular permeability. Thus, the physiologic correlates of changes in tumor K^{trans} following targeted therapy are difficult to pinpoint.

A different class of MRI contrast agents, termed high molecular weight (HMW) agents, has recently become available [36]. These agents are essentially impermeable to endothelial membranes in normal (but not neoplastic) tissues, thus enabling more specific imaging of the tumor and its neovasculature. Furthermore, the permeability of these agents is inversely related to their molecular size, so that with larger agents, endothelial permeability becomes the rate-limiting step in contrast agent transfer into the tumor interstitium. As such, tumor K^{trans} changes in DCE-MRI studies with HMW contrast agents may be a more specific probe of the status of the tumor neovasculature. Furthermore, the slower passage of these agents from blood

to tumor may relax the temporal requirements of DCE-MRI, allowing for more accurate assessment of tumor vascular indices. Several groups have evaluated DCE-MRI using high- vs. low-molecular-weight gadolinium contrast agents to assess tumor response to targeted therapies. In a mouse model of breast cancer, Preda and colleagues [37] demonstrated the superiority of the HMW agent in depicting the early responsiveness of tumor neovasculature to bevacizumab. However, in a similar study of a mouse colon cancer model, both the HMW and LMW contrast agent were effective in determining the early anti-angiogenic effect of sunitinib (SU11248) [38]. It should be noted that there is less experience using HMW contrast agents in humans, with the majority of studies directed toward MR angiography studies [39]. Thus, human studies of the use of HMW agents as probes of tumor angiogenesis are to date lacking.

3.4 Arterial spin labeling MRI

An alternate method for MR-based assessment of tumor perfusion, arterial spin-labeling (ASL) has been proposed [40, 41]. In ASL-MRI, radiofrequency pulses are used to magnetically label the blood flowing into a specific tissue volume. The advantage of this methodology over those using exogenous contrast agents is that the experiment can be repeated sequentially over time or for multiple lesions. Furthermore, the use of magnetically labeled water as a tracer allows for direct measurement of tumor or tissue perfusion. ASL-MRI has been used with great success in brain imaging, allowing for assessment of brain function or as a means of evaluating blood flow alterations in stroke patients [42, 43]. ASL-MRI has been used to evaluate benign brain tumors [44] and ASL-MRI has been shown to correlate with tumor grade in gliomas [45].

ASL-MRI has also been proposed as a means of assessing tumor perfusion outside the brain. For example, Boss and colleagues used ASL-MRI to assess for local relapse of renal cell carcinoma (RCC) after treatment by radiofrequency ablation [46]. De Belazaire and colleagues demonstrated perfusion changes in metastatic RCC treated with PTK/ZK [47]. However, ASL techniques are not routinely available across all imaging centers, and the reliability of this method for vascular assessment of tissues outside of the brain has not been thoroughly evaluated.

3.5 Blood oxygen level dependent-MRI

Blood oxygen level dependent (BOLD)-MRI is another MRI technique that can be used to interrogate the physiology of tumors without exogenous contrast. BOLD imaging takes advantages of subtle differences in magnetic susceptibility between oxy- and deoxy-hemoglobin to assess tissue blood oxygen levels [48]. The technique has been extremely useful in functional MRI (fMRI) studies of brain activation in neuroimaging [49–51]. BOLD-MRI has also been used as an indirect means to evaluate renal perfusion [52–55].

Given the importance of tumor hypoxia in responsiveness to certain therapies (e.g. radiation therapy) BOLD techniques have been proposed as a mean of assaying tumor oxygenation *in vivo* prior to or during therapy [56]. However, given the relative subtle changes in image signal intensity in BOLD imaging, oxygen augmentation techniques through breathing of carbogen or 100% oxygen are generally employed for tumor assessment [57, 58]. Furthermore, given the complex interplay of tumor metabolism and perfusion, the relationship between alterations in tumor vasculature (e.g. vascular shutdown vs. vascular maturation) and BOLD signal changes is likely to be complex. Nevertheless, BOLD-MRI has been used successfully in tumor xenographs to demonstrate the relationship between non-invasive tissue oxygen assessment and histologic measures of tumor vascular maturation [59]. As is true for ASL-MRI, the use of BOLD-MRI as a means of assaying the tumor neovasculature non-invasively will require additional investigation. Nevertheless, the appeal of non-contrast dependent methods such as ASL- and BOLD-MRI to offer high-resolution function imaging of tumors over short time periods may be particularly appealing, especially in studies of VDAs with relatively short time courses of action and rapidly reversible effects.

4 Perfusion CT methods

As with MRI, dynamic contrast enhanced CT can be used to assess the status of tumor neovasculature non-invasively. Many aspects of dynamic contrast-enhanced CT (DCE-CT) make it an attractive alternative to DCE-MRI. In CT, the relationship between iodinated contrast tissue concentration and tissue image intensity is linear, thus simplifying quantification of dynamically enhanced image sets. Unlike MRI, CT image intensity is more uniform within an imaging volume, and CT intensity measures are standardized (Hounsfield units), facilitating comparison across multiple imaging systems. Initial use of CT perfusion in brain imaging for stroke patients was suggested using deconvolution methods to assess blood volume (*rCBV*), blood flow (*rCBF*), and mean transit time (*MTT*) of contrast [60]. Several additional methodologies for obtaining and analyzing CT perfusion images using more complex models have been applied [61–64].

With the widespread application of CT perfusion in stroke imaging, multiple commercial software packages for analysis of CT perfusion images exist which can produce

standardized kinetic terms (blood flow, blood volume, mean transit time), possibly facilitating use in multi-site clinical studies of targeted therapies. However, several factors limit the utility of CT perfusion outside of specialized areas such as the brain. The fixed axial plane of CT scanning may hinder CT-perfusion studies in moving areas of the body (e.g. liver and lung). The relatively high radiation dosages of abdominal CT limit the number of high-quality images that can be obtained repetitively without exposing the patient to unacceptably high radiation levels. Contraindications to iodinated contrast may also restrict the number of patients who may undergo these studies.

Nevertheless, several groups have successfully used CT perfusion in humans to assess and track changes in tumor neovasculature outside of the brain. CT perfusional measures have been shown to correlate with tumor hypoxia in cervical cancer [65], similar to early studies using heuristic evaluation of DCE-MRI enhancement curves to correlate cervical cancer vascularity and predict responsiveness to radiation therapy [66]. CT perfusion has also been used to demonstrate responsiveness of rectal carcinoma to combination chemoradiation [67] and the early response of the rectal tumor neovasculature to bevacizumab [68]. Two separate studies have addressed the use CT perfusion metrics prior to treatment to predict responsiveness of squamous cell cancer of the head and neck to induction chemotherapy [69] and esophageal cancers to neoadjuvant chemotherapy [70], suggesting a potential role of DCE-CT in patient stratification in treatment trials.

5 Nuclear medicine imaging methods

PET and single photon emission computed tomography (SPECT), are nuclear medicine techniques which rely on the emission of energy from exogenously administered radioactive tracers. Tracer concentrations are typically very small—on the order of picomolar—and are thus able to interrogate *in vivo* physiology without significantly altering the function of the system. SPECT images derive from the emission of a single photon by a decaying isotope, and utilize collimators to filter scattered photons and improve image resolution. PET images rely upon the creation of co-incident 511 keV gamma rays originating from the annihilation between the emitted positron and a neighboring electron. The co-incident detection of the paired gamma rays localizes the origin of these photons within the patient's body, constituting the image. PET has greater sensitivity compared with SPECT [71], and has become the modality of choice for functional tissue assessment when a suitable positron emitting tracer is available.

In PET imaging, tracer uptake is indicated by the standardized uptake value (SUV), a measure of mean tissue tracer concentration relative to the mean whole body tracer concentration [72]. ^{18}F-Fluorodeoxyglucose (FDG) is the best studied PET radiotracer. FDG-PET images demonstrate the relative glucose uptake and metabolism of various tissues in the body. Image quantification in FDG-PET is based on user-defined detection of hypermetabolic tumor foci, with the maximal SUV pixel (SUV_{max}) being reported from a tumor region-of-interest. Several elements can lead to variations in SUV_{max} measurements, such as biological (e.g. perfusion, endogenous substrate/transmitter competition), physical (e.g. activity administered, partial volume effect) and technological factors (e.g. differences in scanner and software platforms). One cross-platform phantom and human study for FDG-PET suggests that test-retest differences in SUV may be as high as 15% [73].

Advantages of both SPECT and PET imaging include the relative sensitivity of the technique to very small concentration of tracers and the ease in which image quantitative measures may be derived. Previously, image resolution has been pointed to as one of the drawbacks of emission imaging. However, the advent co registration of functional and anatomic images with hybrid SPECT-CT [74] and PET-CT systems [75], along with recent improvements in PET technology, such as time-of-flight reconstruction [76], have helped to overcome this limitation.

While FDG-PET remains the mainstay of clinical PET imaging in oncology, many other PET or SPECT tracers are available. The choice of radiotracer alters the functional aspects of the resulting images, depicting various biologic or physiologic aspects of the tumor(s). Thus, PET/SPECT imaging can be used to directly evaluate a variety of parameters relating to tumor neovasculature. Including direct evaluation of hemodynamic parameters (blood flow, blood volume), tissue properties (glucose metabolism, hypoxia) or tissue expression of specific markers of angiogenesis (e.g. VEGF, $\alpha v\beta^3$ integrins).

5.1 PET imaging of tumor hemodynamic parameters

Blood volume imaging with PET is performed through the labeling of red blood cells (RBC). The subjects inhale a small volume of ^{11}C or ^{15}O labeled carbon monoxide (CO), resulting in the production of radiolabelled carboxyhemoglobin within RBCs. These labeled RBCs become blood pool tracers, enabling accurate blood volume determination of tumors. Blood volume determination with either ^{11}C– or ^{15}O–CO PET has proved to be a reliable and reproducible method [77, 78]. Blood flow imaging with PET is performed through the direct injection of ^{15}O-labeled water ($^{15}O–H_2O$) [79] or inhalation of carbon dioxide ($^{15}O–CO_2$), the latter tracer being converted in the blood stream to ^{15}O–water through the action of carbonic anhydrase [80]. $^{15}O–H_2O$ imaging has been proven to be a

highly sensitive and reproducible method to evaluate perfusion of both normal and cancerous tissues [81, 82]. However, the short half-life of currently limits the availability of these techniques to imaging centers with ^{15}O production facilities.

5.2 Clinical applications of blood flow and blood volume PET studies

Blood flow and volume of distribution were measured with ^{15}O–H_2O in patients with breast cancer and were shown to be significantly different between malignant and normal tissue [83]. Blood flow also correlated with washout of ^{99m}Tc-Sestamibi, a marker of p-glycoprotein activity, indicative of resistance to chemotherapy (Mankoff et al.) [84, 85].

Changes in tumor blood flow have been used to monitor therapeutic effects of cytotoxic chemotherapy in humans after 2 months of therapy. Mankoff and colleagues used both FDG and ^{15}O–H_2O PET to study patients with locally advanced breast cancer undergoing different neoadjuvant chemotherapy regimens, most doxorubicin based [85]. It was found that both resistant and responsive tumors had an average decline in metabolic activity. Non-responding tumors, however, had an increase in blood flow after the chemotherapy. Lack of decline in blood flow after 2 months of therapy predicted poorer disease-free and overall survival (Fig. 2). In a randomized phase II study evaluating effects of doxorubicin and docetaxel in patients with breast cancer, ^{15}O–H_2O, ^{11}C–CO, and FDG were used to evaluate flow, blood volume and metabolic activity, respectively. Blood flow and glucose metabolism were not shown to correlate with clinical response, as both of these indices decreased in virtually all patients after therapy. However, it was shown that the baseline tumor blood volume of patients who went on to complete pathologic responders (pCR) was slightly lower than those who did not exhibit pCR. Furthermore, post-treatment tumor blood volume remained stable in responding patients, but tended to increase after therapy in patients without pCR [86].

In a pilot study of patients with androgen-independent prostate cancer treated with thalidomide, Kurdziel and colleagues evaluated changes in blood flow, blood volume, and metabolic activity 2 months after therapy. The authors found a strong positive correlation between changes in FDG uptake and changes in PSA, and a moderately positive correlation between changes in blood volume and changes in the PSA. Surprisingly, the authors found negative correlations between changes in blood flow versus changes in FDG uptake. This might be explained by the fact that hypoxic tumors overexpress HIF-1, which in turn upregulates the expression of Glut-1 transporters, a key factor in FDG uptake [87].

Several investigators have evaluated PET to monitor tumor changes in anti-angiogenic therapies. In a phase I trial of human recombinant endostatin, Herbst and colleagues found that ^{15}O–H_2O PET demonstrated decreases in tumor blood flow in the absence of morphologic tumor regression. The authors also found that those changes persisted up to 84 days after the administration of the drug, along with decreased metabolic activity [88]. Lara and colleagues used FDG and ^{15}O–H_2O PET as part of the phase I trial of SU5416—an inhibitor of VEGF-mediated signaling—plus interferon alpha in patients with advanced renal cell carcinoma. Only five subjects underwent both baseline and post-treatment PET studies. In these patients, tumor metabolism and perfusion were unchanged or decreased in four patients with stable disease or minimal response, whereas it increased in the one patient with disease progression [89].

Anderson and colleagues evaluated tumor perfusion, volume of distribution of water and blood volume in patients with inoperable RCC treated with razoxane, a chemotherapeutic agent which inhibits cell division in early mitotic phases and also has anti-angiogenic properties. The authors found that overall there was no statistically significant correlation between changes in tumor perfusion and clinical response after 4–8 weeks of therapy. However, significant perfusional changes were seen in selected patients whose tumors demonstrated

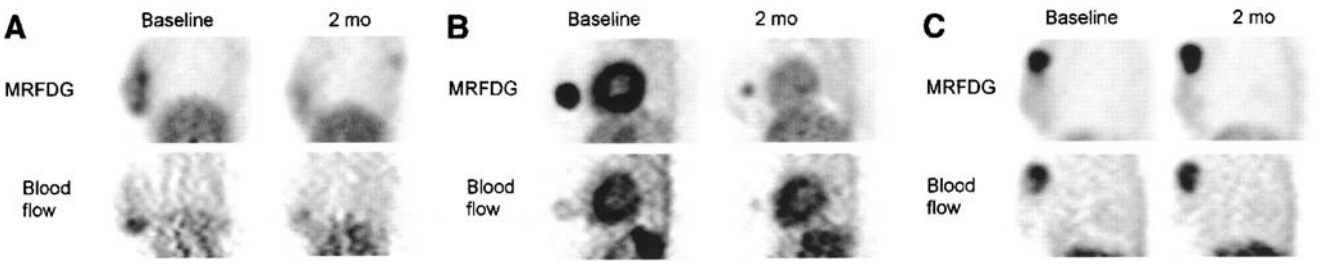

Fig. 2 Sagittal images of breast and chest of patients with locally advanced breast cancer, before therapy (*left*) and after 2 months of therapy (*right*) showing ^{18}F-FDG and ^{15}O-water uptake. Patient with macroscopic complete response (**A**), patient with partial (**B**), and patient with no response (**C**) are shown (Reprinted from [84 85] Changes in blood flow and metabolism in locally advanced breast cancer treated with neoadjuvant chemotherapy. J Nucl Med. Volume 44. 2003. p 1806–14, with permission)

higher pretreatment levels of perfusion, whereas no such changes were seen in patients with lower native tumor perfusion [90].

The effects of vascular disruptive agents can also be tracked with PET imaging. Anderson and colleagues used $^{15}O–H_2O$ and $^{15}O–CO$ PET in a phase I clinical trial of CA4P, in patients with advanced solid tumors. There was shown to be significant reduction in tumor blood flow 30 min after treatment, an effect that persisted after 24 h in patients receiving larger doses of CA4P. Tumor blood volume also demonstrated a significant decrease 30 min after CA4P, also with a return to baseline values at 24 h (although no dose dependence in blood volume changes were noted) [91]. Although there was no correlation of PET indices with clinical responses, this study shows the feasibility of using PET to evaluate vascular pharmacodynamics in a dose-escalation phase I study. The PET information was used then to help determine the optimal CA4P dose for subsequent phase II trials.

Logan and colleagues evaluated the effects of IL-1 in tumor blood flow in a phase I trial of IL-1 and carboplatin in patients with solid malignancies metastatic to lung. At 2 h after the administration of IL-1, there was significant decrease in tumor blood flow assessed with PET. Where IL-1 also caused decrease in systemic blood pressure, the effects on tumor blood flow persisted until 4 h after treatment, when the patients became normotensive (Logan et al.) [92].

5.3 PET imaging of tumor hypoxia

Hypoxia results from the imbalance between supply and consumption of oxygen and is a temporarily and spatially heterogeneous process. There are three main pathogenic mechanisms in the development of hypoxia in solid tumors: (a) perfusion, secondary to the abnormalities in the tumor neovasculature; (b) diffusion, related with the tumor's distorted geometry and (c) anemia, either tumor-associated or therapy induced. Therefore, while tumor hypoxia itself is not a direct marker of the status of tumor neovasculature, alterations in tumor vascular physiology may be expected to influence the presence and degree of tumor hypoxia. In cancer patients, hypoxia may predict response to (chemo-therapy) radiation therapy and ultimately the outcome of the disease. In cervical [93, 94] head and neck cancer [95–99], and soft tissue sarcomas [95–98] the presence of tumor hypoxia is associated with a poor prognosis. The interplay between tumor perfusion, tumor neovascular maturation, and tumor hypoxia is therefore likely to be an important metric for determining prognosis and tumor responsiveness in chemoradiation treatment regimens.

Currently, polarographic oxygen electrode measurements of tissue oxygenation are considered the gold standard for measuring tumor oxygenation. In addition to being an invasive method, electrode measurements do not provide a full map of the tumor oxygenation, and measurements are limited to tissues accessible for electrode placement. These limitations have prompted research evaluating non-invasive techniques for imaging oxygen distribution in tumors. The most studied PET radiotracers for hypoxia imaging are ^{18}F-Fluoromisonidazole (FMISO), ^{18}F-EF5, ^{18}F-FAZA (the 2-nitroimidazoles) and Copper (II) diacetyl-bis(N4)-methylthiosemicarbazone (Cu-ATSM). These radiotracers selectively target viable, but hypoxic cells. In their oxygenated states, these tracers are freely diffusion into the tissues. However, when localized within hypoxic tissues, tracer reduction occurs, in each case converting these tracers into non-diffusible forms which are then trapped within the hypoxic tissue. In tissues with normal oxygen tension, the tracers remain oxidized and can diffuse back to the extracellular compartment [100].

Several studies have used PET imaging to track tumor hypoxia prior to or during treatment. Rischin et al. [101] showed that hypoxia on FMISO PET was associated with a high risk of locoregional failure in patients with head and neck cancer receiving a chemoradiotherapy regimen without tirapazamine. In lung cancer patients undergoing chemo-radiation [102], a decrease in FMISO uptake from the baseline, indicating tumor reoxygenation, was associated with better tumor response. On the other hand, increase or nearly unchanged tracer uptake corresponded to worse local tumor outcomes.

While no studies have directly evaluated tumor hypoxia in the setting of vascular targeted therapies, several studies have evaluated the correlation between tumor hypoxia and markers of tumor angiogenesis. In a study of malignant gliomas, FMISO uptake was shown to correlate with increased metabolic activity as well as with VEGF-R1 and Ki-67 expression, markers of angiogenesis and cell proliferation, respectively [103]. Bruehlmeier and colleagues [104] studied FMISO and $^{15}O–H_2O$ PET in glioma patients, demonstrating a positive correlation between early FMISO uptake with blood flow images. This correlation, however, was no longer present in the delayed FMISO images, when FMISO retention more directly reflected the degree of tumor hypoxia. The authors also found that hypoxia was associated with tumor hypoperfusion in only two patients, whereas in four other patients, hypoxia was found in tumor areas with intermediate to high perfusion. These findings restate the multifactorial nature of hypoxia in solid tumors and indicate that tumor hypoxia can result even in the absence of image-assessed low tumor perfusion.

A novel approach in imaging hypoxia has been to evaluate its effects on cell markers. In tissues with low partial pressures of oxygen, hypoxia inducible factor α (HIF1α) mediates a complex cascade of events. Carbonic

anhydrase 9 (CA9) is one of the genes upregulated via HIF1α, and has been implicated in the maintenance of intracellular pH [105]. cG250, a chimeric antibody against CA9, has been developed and labeled with Iodine-131 [106], Indium-111 [107] and Technetium-99m [108] for immunoscintigraphy as well as radioimmunotherapy [109]. Recently, cG250 has been labeled with Iodine-124, a positron emitter, and it was shown in a prospective trial to correlate with CA9 expression. ^{124}I-cG250 was shown to have sensitivity of 94% and specificity of 100% in the detection of clear cell phenotype in patients with renal cell carcinoma [110]. Quantification of CA9 expression with ^{124}I-cG250 therefore represents a promising strategy to interrogate tumor hypoxia before and during treatment with targeted agents.

5.4 Glucose metabolism and tumor perfusion

FDG is the most commonly used tracer in oncologic PET and is the only oncologic PET tracer approved by the Food and Drug Administration for routine clinical use. FDG-PET imaging is based on the increased glucose metabolism by cancer cells [111]. The tracer is taken up by the glucose transporters, undergoes phosphorylation by hexokinase, but does not undergo any further metabolism and thus remains trapped within the cell.

Therefore, while FDG is the prototypic metabolic radiotracer, some studies have suggested that tumor FDG uptake may be linked closely to tumor angiogenesis. Bos and colleagues found that in breast cancer, FDG uptake correlates not only with glucose transporter and hexokinase expression, but also with microvessel density. [112] Zasadny and colleagues found a close correlation between FDG uptake and blood flow in breast cancers. However, in regions of lower tumor blood flow, the slope of the FDG uptake curve was higher, possibly representing increased anaerobic metabolism in areas of poor tumor perfusion [113]. Thus, the relationship between tumor glucose metabolism and tumor perfusion may be a complex one, and it is not clear that alterations in tumor neovasculature will be easily correlated to changes in tumor FDG uptake.

5.5 PET and SPECT imaging of angiogenesis markers

5.5.1 Vascular endothelial growth factor

Vascular endothelial growth factor (VEGF) is one of the principal cytokines involved in angiogenesis, regulating blood vessel proliferation and permeability, as well as serving as an anti-apoptotic factor for the newly formed blood vessels. Preliminary studies have demonstrated the feasibility of labeling VEGF with SPECT agents or positron emitters to detect tumors. In 40 patients with gastrointestinal tumors, SPECT and planar imaging with ^{123}I labeled VEGF-165 yielded an overall tumor detection rate of 58% [114]. Jayson and colleagues utilized the positron emitting ^{124}I labeled huMV833 to evaluate the biodistribution and clearance of the unlabeled humanized anti-VEGF antibody huMV833 in a phase I clinical trial in patients with advanced solid tumors [115]. Cai and colleagues successfully demonstrated the ability of Copper-64-DOTA-$VEGF_{121}$ to image vascular endothelial growth factor expression *in vivo* [116]. Hsu and colleagues used ^{64}Cu-DOTA-$VEGF_{121}$ fused with the recombinant plant toxin gelonin (rGel) for both imaging and treatment in animal tumors. The authors found that ^{64}Cu-DOTA-$VEGF_{121}$/rGel was able to image VEGF receptor expression and also cause tumor neovascular damage [117].The iodinated IgG1 monoclonal antibody against VEGF, ^{124}I-VG76e, demonstrated good tumor localization in fibrosarcoma xenographs [118]. However, it has not been studied in anti-angiogenic therapy evaluation.

Given these early results, targeting VEGF and VEGF receptor expression as a means of monitoring the effects of anti-angiogenic therapy would appear to be an attractive option. However, quantitative VEGF/VEGF-R targeting has not to date been evaluated as a marker of tumor angiogenic activity in human therapeutic trials.

5.5.2 Integrin Alpha-v-Beta-3

Integrins are a family of transmembrane molecules which mediate numerous cell-cell and cell-matrix interactions, such as cell adhesion, proliferation and apoptosis of tumor cells and of activated endothelial cells. One prominent member of this receptor class is integrin αvβ3, which is highly expressed in endothelial cells during angiogenesis. Its expression in normal vasculature and other organs, however is weak. A common feature to many members of the integrin family binding of the tripeptidic sequence Arg-Gly-Asp (RGD). Radiolabeled RDG peptide imaging therefore constitutes a promising strategy to evaluate integrin expression *in vivo* and to serve as a non-invasive means of assessing tumor neovasculature.

Sivolapenko and colleagues, used Technetium-99 m-RGD to evaluate patients with metastatic melanoma [119] demonstrating detection sensitivity of 77.3%, including 75% of the lymph node metastasis and all the solid organ metastasis. PET imaging with ^{18}F-Galacto-RGD has been used to evaluate angiogenesis, demonstrating significant correlation between radiotracer accumulation and αvβ3 receptor density by immunohistochemistry and Western blot in animal tumor models [120]. Beer at al found strong correlations between radiotracer uptake and imunohistochemistry staining intensity of αvβ3 vessels [121]. ^{18}F-Galacto-RGD was used to non-invasively monitor tumor growth and angiogenesis in

mice with gliobastoma multiforme [122]. Jung and colleagues [123], used a novel ^{99m}Tc-RDG compound—Glucosamino $^{(99m)}$Tc-d-c(RGDfK)—to image fibrosarcoma and lung carcinoma xenographs. In addition to the favorable integrin imaging characteristics, the authors also found that in mice treated with paclitaxel there was decreased radiotracer uptake. This finding was associated with delayed tumor growth as well as decreased tumor alpha(v)beta3 integrin expression.

6 Ultrasound methods

Ultrasonography (US) utilizes high frequency sound ways to produce images. Alterations in tissue acoustic properties create interfaces that reflect the emitted sound waves, which are then received back by the transmitter. The time delay between sound wave emission and detection correlates with the depth of the various reflected surfaces.

Vascular depiction in US can be achieved through of Doppler imaging to detect moving reflectors, representing the surfaces of red blood cells in flowing blood. Thus, vascular-based imaging through various Doppler techniques (color, power, etc.) is a routine methodology for identifying and depicting pathology in large vessels. However, flow-sensitivity limits the ability of Doppler US to identify vessels smaller than approximately 50 μm [124]. Nevertheless, large feeding vessels in tumors can be reliably imaged by Doppler US methods, and qualitative Doppler US assessment can be used as an adjunct in the detection and characterization of malignant breast and prostate lesions [125, 126].

The advent of microbubble contrast agents has greatly improved the ability of US to probe tumor vascular architecture. US microbubble contrast agents are on the order of 1–10 μm in diameter. The bubbles consist of a gas center (usually air or a perfluoronated hydrocarbon), with a shell of variable composition (lipid, protein, or polymer) [127]. These agents remain entirely intravascular. However, their high reflective index increases the relative US signal in both gray scale and Doppler modes. The addition of an US contrast agent with specialized imaging techniques (e.g. pulsed inversion imaging) can effectively decrease the minimal vessel size depicted by US. As such, quantitative US imaging can be used to interrogate the status of tumor neovasculature. Furthermore, the transmitted US wave can be used to intermittently destroy the contrast agent in a focal region of tissue. Repetitive cycles of destruction/detection can be put into place such that the rate of new contrast agent entry into the tissue of interest can be measured as a gauge tumor blood flow.

Quantitation schemes for assessing tumor vascularity from US images vary. Doppler US images may be assessed for total number of pixels with flow, weighted by the relative or absolute flow velocities [128, 129]. Similar schemes can be applied with contrast-enhanced images. Blood flow measures may be estimated with or without intermittent bubble destruction [130–132]. However, reproducibility studies in humans are to date lacking and the use of US techniques to interrogate the tumor neovasculature and the effects of targeted therapy have been performed mostly in animal studies.

Nevertheless, both contrast-enhanced and non-enhanced US can be used to depict tumor vascular alterations in humans undergoing anti-vascular therapies [133]. Berlottoto and colleagues demonstrated decreases in tumor blood flow and volume in human hepatocellular carcinoma (HCC) 15 days after administration of thalidomide [131]. In another study of thalidomide in HCC [134], higher tumor vascular indices pre treatment were predictive of response, and marked decreases in tumor vascular indices were seen in 4/5 patients with subsequent objective tumor response by CT. Given the wide availability of US, and the potential for repetitive assessment of tumor vascularity, the use of US as a probe of human tumor vasculature in vascular targeted therapies is expected to increase. However, standard quantitation methods are needed, especially due to the potential of operator-dependence on resulting quantitation of tumor vascular metrics. Furthermore, tumors within certain anatomic regions (lung, bone) may be less amenable to US interrogation.

7 Optical (Near-IR) imaging methods

Diffuse optical tomography (DOT) is a new imaging tool with great potential to monitor the status of tumor neovasculature and the vascular effects of targeted and non-targeted therapies. DOT utilizes non-ionizing radiation (i.e. near-IR light), evaluating the absorption and scattering patterns of tissues at multiple near-IR wavelengths. DOT evaluation of tumors provides several unique physiologic and hemodynamic parameters, including total hemoglobin concentration, blood oxygen saturation, blood flow, scattering, and tissue water and lipid content [135, 136]. DOT is technologically simple, inexpensive and rapid. It can be used as a portable device, facilitating the bedside evaluation of tumors, and can be performed repeatedly over short intervals, facilitating longitudinal studies of fast acting agents such as VDAs.

The use of optical imaging with exogenously added near-IR absorbers can further enhance the optical contrast of tumors. Currently, Indocyanine Green (ICG) is the only FDA-approved compound suitable for DOT, having an absorption and fluorescence spectra in the near-IR spectral window (600–1,000 nm). Based on absorption [137, 138]

and fluorescence contrast [139], higher concentration of ICG have been shown in breast tumors relative to that of normal tissue, likely due to higher contrast delivery and/or delayed contrast washout.

Despite its advantages, there are current shortcomings to DOT evaluation of tumor in practice. Few centers currently perform DOT studies in humans, and equipment varies between investigators, preventing standardization and hampering comparison of results from different centers. Due to absorption and scattering properties of near-IR light, DOT can only be used to probe tumors that are relatively superficial to the skin surface or an accessible internal cavity (e.g. transrectal optical probes for prostate cancer). Nevertheless, DOT has been successfully used to assess and monitor tumors in a variety of sites in humans, including breast [140–144], head and neck [145], and prostate [146]. These studies demonstrate the reliability of DOT for identifying tumors, and have demonstrated the capability of DOT to monitor physiologic changes in breast tumors after neoadjuvant chemotherapy [140–144] (Fig. 3). With its sensitivity to both tumor perfusion and oxygenation, DOT may be an ideal imaging modality for probing tumors before and during radiation therapy [145] or photodynamic therapy [146]. In addition, DOT has been used to monitor the anti-vascular effects of CA4P in a mouse model of melanoma [147], demonstrating significant decreases in both blood flow and tumor oxygenation 1 h after drug administration.

8 Summary: Implications for tumor vascular assessment in human studies

As we have discussed, a wide range of imaging modalities has been utilized in an attempt to monitor the status of tumor neovasculature in the setting of vascular targeted therapies in human trials. To date, no one method has emerged that satisfies all of the requirements for routine use in human studies.

Several methods exist for direct assessment of tumor vascular physiology. PET studies with labeled water is a promising avenue for tumor vascular assessment, but is limited to sites accessible to cyclotron facilities due to the short half-life of ^{15}O as a positron emitter. DCE-MRI is a methodology that has been applied widely, due to the ease of use with modern MR imaging equipment and the routine availability of gadolinium contrast agents. However, the complexity of MR image intensity standardization, and the non-linear relationship between gadolinium concentration and image enhancement have challenged the ability of the MRI community to devise uniform methods for DCE-MRI image acquisition and quantification. Other high-resolution cross-sectional techniques for assessing tumor neovasculature, such as perfusion-CT and arterial spin-labeled MRI show promise, but remain less well studied that the ^{15}O PET or DCE-MRI techniques.

Other modalities, such as microbubble contrast enhanced US or near-IR optical techniques have been used in selected centers for tumor vascular assessment. These techniques offer several advantages, including portability and the possibility of repeated measures in the setting of treatment with fast acting vascular disruptive agents. However, uniform methodologies have not been devised or tested, and each method may be limited with respect to the anatomic areas accessible for tumor vascular interrogation.

Molecular imaging offers additional promise for assessing tumor angiogenesis through targeting of key molecules involved in the development and maintenance of tumor angiogenesis. However, the ability of these targets to be reproducibly quantified via SPECT or PET imaging remains unknown.

As the role of vascular targeted therapy continues to grow in oncology, there will be increasing demands on the development and deployment of robust non-invasive means of assessing tumor response to these therapies. Therefore, continued incorporation of these imaging methodologies into single- and multi-site clinical trials of targeted agents should be encouraged. However, critical evaluation of the performance of these biomarkers should be mandated. These include testing the repeatability of image-derived metrics, evaluating the robustness of novel imaging protocol implementation across platforms, and determining the true relationship between alteration in image metrics and the degree of neovascular inhibition *in vivo*.

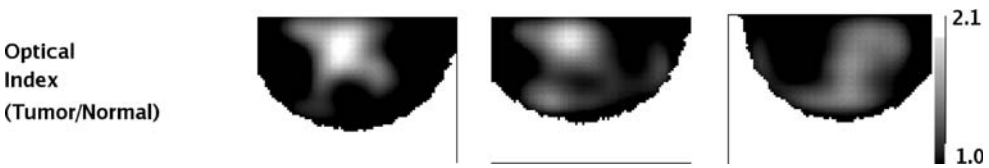

Fig. 3 Representative image slices from DOT of a patient with breast cancer, before and after the first cycle, and after the third cycle of docetaxel. Patient had previously received four cycles of Doxorubicin–Cyclophosphamide as part of the neoadjuvant regimen. Optical index is constructed based on tumor-to-normal ratios of total hemoglobin concentration, blood oxygen saturation and scattering for representative measure of tumor-to-normal ratio. Images demonstrate clear shrinkage and decrease of optical index over time (Personal Data, Regine Choe)

References

1. Carmeliet, P., & Jain, R. K. (2000). Angiogenesis in cancer and other diseases. *Nature*, *407*, 249–257.
2. Hanahan, D., & Weinberg, R. A. (2000). The hallmarks of cancer. *Cell*, *100*, 57–70.
3. O'Connor, J. P., Jackson, A., Parker, G. J., & Jayson, G. C. (2007). DCE-MRI biomarkers in the clinical evaluation of antiangiogenic and vascular disrupting agents. *British Journal of Cancer*, *96*(2), 189–195.
4. Padhani, A. R. (2005). Where are we with imaging oxygenation in human tumours. *Cancer Imaging*, *5*(1), 128–130.
5. Evelhoch, J., Garwood, M., Vigneron, D., Knopp, M., Sullivan, D., & Menkens, A. (2005). Expanding the use of magnetic resonance in the assessment of tumor response to therapy: workshop report. *Cancer Research*, *65*(16), 7041–7044.
6. Leach, M. O., Brindle, K. M., Evelhoch, J., Griffiths, J. R., Horsman, M. R., Jackson, A., et al. (2005). The assessment of antiangiogenic and antivascular therapies in early-stage clinical trials using magnetic resonance imaging: issues and recommendations. *British Journal of Cancer*, *92*(9), 1599–1610.
7. Roberts, C., Buckley, D. L., & Parker, G. J. M. (2006a). Comparison of errors associated with single- and multi-bolus injection protocols in low-temporal-resolution dynamic contrast-enhanced tracer kinetic analysis. *Magnetic Resonance in Medicine*, *56*, 611–619.
8. Henderson, E., Rutt, B. K., & Lee, T. Y. (1998). Temporal sampling requirements for the tracer kinetics modeling of breast disease. *Magnetic Resonance Imaging*, *16*, 1057–1073.
9. Evelhoch, J. (1999). Key factors in the acquisition of contrast kinetic data for oncology. *Journal of Magnetic Resonance Imaging*, *10*, 254–259.
10. Kety, S. S. (1951). The theory and applications of the exchange of inert gas at the lungs and tissues. *Pharmacological Reviews*, *3*, 1–41.
11. Tofts, P. S., Berkowitz, B., & Schnall, M. D. (1995). Quantitative analysis of dynamic Gd-DTPA enhancement in breast tumors using a permeability model. *Magnetic Resonance of Medicine*, *33*, 564–568.
12. Tofts, P. S., Brix, G., Buckley, D. L., Evelhoch, J., Henderson, E., Knopp, M. V., et al. (1999). Estimating kinetic parameters from dynamic contrast-enhanced T(1)-weighted MRI of a diffusable tracer: standardized quantities and symbols. *Journal of Magnetic Resonance Imaging*, *10*, 223–232.
13. Tofts, P. S., & Kermode, A. G. (1991). Measurement of the blood-brain barrier permeability and leakage space using dynamic MR imaging. 1. Fundamental concepts. *Magnetic Resonance in Medicine*, *17*, 357–367.
14. Yankeelov, T. E., Rooney, W. D., Li, X., & Springer, C. S. (2003). Variation of the relaxographic "shutter-speed" for transcytolemmal water exchange affects the CR bolustracking curve shape. *Magnetic Resonance in Medicine*, *50*, 1151–1169.
15. Li, S., Peck-Radosavljevic, M., Kienast, O., Preitfellner, J., Hamilton, G., & Kurtaran, A. (2003). Imaging gastrointestinal tumours using vascular endothelial growth factor-165 (VEGF165) receptor scintigraphy. *Annals of Oncology*, *4*, 1274–1277.
16. Galbraith, S. M., Lodge, M. A., Taylor, N. J., Rustin, G. J. S., Bentzen, S. M., Stirling, J. J., et al. (2002a). Reproducibility of dynamic contrast-enhanced MRI in human muscle and tumours: comparison of quantitative and semi-quantitative analysis. *NMR in Biomedicine*, *15*, 132–142.
17. Lankester, K. J., Taylor, N. J., Stirling, J. J., Boxall, J., d'Arcy, J. A., & Leach, M. O. (2005). Effects of platinum/taxane based chemotherapy on acute perfusion in human pelvic tumours measured by dynamic MRI. *British Journal of Cancer*, *93*, 979–985.
18. Roberts, C., Issa, B., Stone, A., Jackson, A., Waterton, J. C., & Parker, G. J. M. (2006b). Comparative study into the robustness of compartmental modeling and model-free analysis in DCE-MRI studies. *Journal of Magnetic Resonance Imaging*, *23*, 554–563.
19. Morgan, B., Utting, J. F., Higginson, A., Thomas, A. L., Steward, W. P., & Horsfield, M. A. (2006). A simple, reproducible method for monitoring the treatment of tumours Effect of thalidomide in hepatocellular carcinoma: assessment with power doppler US and analysis of circulating angiogenic factors. *Radiology*, *235*, 509–516.
20. Parker, G. J. M., Roberts, C., Macdonald, A., Buonaccorsi, G. A., Cheung, S., & Buckley, D. L. (2006). Experimentally derived functional form for a population-averaged high-temporal-resolution arterial input function for dynamic contrast-enhanced MRI. *Magnetic Resonance in Medicine*, *56*, 993–1000.
21. Knopp, M. V., Brix, G., Junkermann, H. J., & Sinn, H. P. (1994). MR mammography with pharmacokinetic mapping for monitoring of breast cancer treatment during neoadjuvant therapy. *Magnetic Resonance Imaging Clinics of North America*, *2*, 633–658.
22. Mross, K., Drevs, J., Muller, M., Medinger, M., Marme, D., Hennig, J., et al. (2005). Phase I clinical and pharmacokinetic study of PTK/ZK, a multiple VEGF receptor inhibitor, in patients with liver metastases from solid tumours. *European Journal of Cancer*, *23*, 1291–1299.
23. Liu, G., Rugo, H. S., Wilding, G., McShane, T. M., Evelhoch, J. L., Ng, C., et al. (2005). Dynamic contrast-enhanced magnetic resonance imaging as a pharmacodynamic measure of response after acute dosing of AG–013736, an oral angiogenesis inhibitor, in patients with advanced solid tumors: results from a phase I study. [see comment]. *Journal of Clinical Oncology*, *23*(24), 5464–5473.
24. O'Donnell, A., Padhani, A. R., Hayes, C., Kakkar, A. J., Leach, M., Trigo, J. M., et al. (2005). A Phase I study of the angiogenesis inhibitor SU5416 (semaxanib) in solid tumours, incorporating dynamic contrast MR pharmacodynamic end points. *British Journal of Cancer*, *93*(8), 876–883.
25. Xiong, H. Q., Herbst, R., Faria, S. C., Scholz, C., Davis, D., Jackson, E. F., et al. (2004). A phase I surrogate endpoint study of SU6668 in patients with solid tumors. *Investigational New Drugs*, *22*(4), 459–466.
26. Thomas, A. L., Morgan, B., Horsfield, M. A., Higginson, A., Kay, A., & Lee, L. (2005). Phase I study of the safety, tolerability, pharmacokinetics, and pharmacodynamics of PTK787/ZK 222584 administered twice daily in patients with advanced cancer. *Journal of Clinical Oncology*, *23*(18), 4162–4171.
27. Morgan, B., Thomas, A. L., Drevs, J., Hennig, J., Buchert, M., Jivan, A., et al. (2003). Dynamic contrast-enhanced magnetic resonance imaging as a biomarker for the pharmacological response of PTK787/ZK 222584, an inhibitor of the vascular endothelial growth factor receptor tyrosine kinases, in patients with advanced colorectal cancer and liver metastases: results from two phase I studies.[see comment]. *Journal of Clinical Oncology*, *21*, 3955–3964.
28. Wedam, S. B., Low, J. A., Yang, S. X., Chow, C. K., Choyke, P. L., Danforth, D., et al. (2006). Antiangiogenic and antitumor effects of bevacizumab in patients with inflammatory and locally advanced breast cancer. *Journal of Clinical Oncology*, *24*(5), 769–777.
29. ODwyer, P. J., Rosen, M., Gallagher, M., Schwartz, B., & Flaherty, K. T. (2005). Pharmacodynamic study of BAY 43–9006 in patients with metastatic renal cell carcinoma. *Journal of Clinical Oncology/ 2005 ASCO Annual Meeting Proceedings*, *23*, 3005.
30. Hahn, O., Yeng, C., Medved, M., Karczmar, G. S., Kistner, E., & Manchen, B. (2007). Dyamic contrast enhanced MRI (DCE-MRI)

pharmacodynamic (PD) study of sorafenib in metastatic renal cell carcinoma (RCC): Results of a randomized, phase II trial. *Journal of Clinical Oncology/ 2007 ASCO Annual Meeting Proceedings*, *25*, 3545.
31. Galbraith, S. M., Rustin, G. J. S., Lodge, M. A., Taylor, N. J., Stirling, J. J., & Jameson, M. (2002b). Effects of 5,6-dimethylxanthenone-4-acetic acid on human tumor microcirculation assessed by dynamic contrast-enhanced magnetic resonance imaging. *Journal of Clinical Oncology*, *20*, 3826–3840.
32. Dowlati, A., Robertson, K., Cooney, M., Petros, W. P., Stratford, M., Jesberger, J., et al. (2002). A phase I pharmacokinetic and translational study of the novel vascular targeting agent combretastatin a-4 phosphate on a single-dose intravenous schedule in patients with advanced cancer. *Cancer Research*, *62*, 3408–3416.
33. Galbraith, S. M., Maxwell, R. J., Lodge, M. A., Tozer, G. M., Wilson, J., & Taylor, N. J. (2003). Combretastatin A4 phosphate has tumor antivascular activity in rat and man as demonstrated by dynamic magnetic resonance imaging. *Journal of Clinical Oncology*, *21*(15), 2831–2842.
34. Stevenson, J. P., Rosen, M. A., Sun, W., Gallagher, M., Haller, D. G., Vaughn, D., et al. (2003). Phase I trial of the antivascular agent combretastatin A4 phosphate on a 5-day schedule to patients with Rosen, MS 43 cancer: magnetic resonance imaging evidence for altered tumor blood flow. *Journal of Clinical Oncology*, *21*(23), 4428–4438.
35. Evelhoch, J. L., LoRusso, P. M., He, Z., DelProposto, Z., Polin, L., Corbett, T. H., et al. (2004). Magnetic resonance imaging measurements of the response of murine and human tumors to the vasculartargeting agent ZD6126. *Clinical Cancer Research*, *10*(11), 3650–3657.
36. Barrett, T., Kobayashi, H., Brechbiel, M., & Choyke, P. L. (2006). Macromolecular MRI contrast agents for imaging tumor angiogenesis. *European Journal of Radiology*, *60*, 353–366.
37. Preda, A., Novikov, V., Moglich, M., Turetschek, K., Shames, D. M., & Brasch, R. C. (2004). MRI monitoring of Avastin antiangiogenesis Rosen, MS 42 therapy using B22956/1, a new blood pool contrast agent, in an experimental model of human cancer. *Journal of Magnetic Resonance Imaging*, *20*, 865–873.
38. Marzola, P., Degrassi, A., Calderan, L., Farace, P., Nicolato, E., Crescimanno, C., et al. (2005). Early antiangiogenic activity of SU11248 evaluated *in vivo* by dynamic contrast-enhanced magnetic resonance imaging in an experimental model of colon carcinoma. *Clinical Cancer of Research*, *11*, 5827–5832.
39. Goyen, M., Edelman, M., Perreault, P., O'Riordan, E., Bertoni, H., Taylor, J., et al. (2005). MR angiography of aortoiliac occlusive disease: a phase III study of the safety and effectiveness of the bloodpool contrast agent MS-325. *Radiology*, *236*, 825–833.
40. Detre, J. A., & Alsop, D. C. (1999). Perfusion magnetic resonance imaging with continuous arterial spin labeling: methods and clinical applications in the central nervous system. *European Journal of Radiology*, *30*(2), 115–124.
41. Alsop, D. C., & Detre, J. A. (1998). Multisection cerebral blood flow MR imaging with continuous arterial spin labeling. *Radiology*, *208*, 410–416.
42. Wintermark, M., Sesay, M., Barbier, E., Borbely, K., Dillon, W. P., Eastwood, J. D., et al. (2005). Comparative overview of brain perfusion imaging techniques. *Stroke*, *36*(9), e83–e99.
43. Wolf, R. L., & Detre, J. A. (2007). Clinical neuroimaging using arterial spin-labeled perfusion magnetic resonance imaging. *Neurotherapeutics*, *4*(3), 346–359.
44. Kimura, H., Takeuchi, H., Koshimoto, Y., Arishima, H., Uematsu, H., & Kawamura, Y. (2006). Perfusion imaging of meningioma by using continuous arterial spin-labeling: comparison with dynamic susceptibility-weighted contrastenhanced MR images and histopathologic features. *American Journal of Neuroradiology*, *27*(1), 85–93.
45. Wolf, R. L., Wang, J., Wang, S., Melhem, E. R., O'Rourke, D. M., & Judy, K. D. (2005). Grading of CNS neoplasms using continuous arterial spin labeled perfusion MR imaging at 3 Tesla. *Journal of Magnetic Resonance Imaging*, *22*(4), 475–482.
46. Boss, A., Martirosian, P., Schraml, C., Clasen, S., Fenchel, M., & Anastasiadis, A. (2006). Morphological, contrast-enhanced and spin labeling perfusion imaging for monitoring of relapse after RF ablation of renal cell carcinomas. *European Radiology*, *16*(6), 1226–1236.
47. De Bazelaire, C., Rofsky, N. M., Duhamel, G., Michaelson, M. D., George, D., & Alsop, D. C. (2005). Arterial spin labeling blood flow magnetic resonance imaging for the characterization of metastatic renal cell carcinoma(1). *Academic Radiology*, *12* (3), 347–357.
48. Logothetis, N. K., & Pfeuffer, J. (2004). On the nature of the BOLD fMRI contrast mechanism. *Magnetic Resonance Imaging*, *22*(10), 1517–1531.
49. Hillis, A. E. (2007). Magnetic resonance perfusion imaging in the study of language. *Brain & Language*, *102*(2), 165–175.
50. Gaillard, W. D., Grandin, C. B., & Xu, B. (2001). Developmental aspects of pediatric fMRI: considerations for image acquisition, analysis, and interpretation. *Neuroimage*, *13*, 239–249.
51. Mattay, V. S., & Weinberger, D. R. (1999). Organization of the human motor system as studied by functional magnetic resonance imaging. *European Journal of Radiology*, *30*(2), 105–114.
52. Thoeny, H. C., Zumstein, D., Simon-Zoula, S., Eisenberger, U., De Keyzer, F., Hofmann, L., et al. (2006). Functional evaluation of transplanted kidneys with diffusion-weighted and BOLD MR imaging: initial experience. *Radiology*, *241*, 812–821.
53. Prasad, P. V. (2006). Evaluation of intra-renal oxygenation by BOLD MRI. *Nephron clinical practice*, *103*(2), c58–c65.
54. dos Santos, E. A., Li, L., Ji, L., & Prasad, P. V. (2007). Early changes with diabetes in renal medullary hemodynamics as evaluated by fiberoptic probes and BOLD magnetic resonance imaging. *Investigative Radiology*, *42*(3), 157–162.
55. Prasad, P. V., & Priatna, A. (1999). Functional imaging of the kidneys with fast MRI techniques. *European Journal of Radiology*, *29*(2), 133–148.
56. Robinson, S. P., Howe, F. A., Rodrigues, L. M., Stubbs, M., & Griffiths, J. R. (1998). Magnetic resonance imaging techniques for monitoring changes in tumor oxygenation and blood flow. *Seminars in Radiation Oncology*, *8*(3), 197–207.
57. Rijpkema, M., Kaanders, J. H. A. M., Joosten, F. B. M., van der Kogel, A. J., & Heerschap, A. (2002). Effects of breathing a hyperoxic hypercapnic gas mixture on blood oxygenation and vascularity of head-and-neck tumors as measured by magnetic resonance imaging. *International Journal of Radiation Oncology, Biology, Physics*, *53*(5), 1185–1191.
58. Taylor, N. J., Baddeley, H., Goodchild, K. A., Powell, M. E., Thoumine, M., Culver, L. A., et al. (2001). BOLD MRI of human tumor oxygenation during carbogen breathing. *Journal of Magnetic Resonance Imaging*, *14*, 156–163.
59. Gilead, A., Meir, G., & Neeman, M. (2004). The role of angiogenesis, vascular maturation, regression and stroma infiltration in dormancy and growth of implanted MLS ovarian carcinoma spheroids. *International Journal of Cancer*, *108*, 524–531.
60. Axel, L. (1980). Cerebral blood flow determination by rapid-sequence computed tomography: theoretical analysis. *Radiology*, *137*, 679–686.
61. Dawson, P. (2006). Functional imaging in CT. *European Journal of Radiology*, *60*(3), 331–340.
62. Laking, G. R., West, C. M. L., Buckley, D. L., Matthews, J., & Price, P. M. (2006). Imaging vascular physiology to monitor cancer treatment. *Critical Oncology Hematology*, *58*(2), 95–113.

63. Miles, K. A. (2003). Perfusion CT for the assessment of tumour vascularity: which protocol. *British Journal of Radiology*, *76*, S36–S42.
64. Bisdas, S., Konstantinou, G. N., Lee, P. S., Thng, C. H., Wagenblast, J., & Baghi, M. (2007). Dynamic contrast-enhanced CT of head and neck tumors: perfusion measurements using a distributed-parameter tracer kinetic model. Initial results and comparison with deconvolution-based analysis. *Physics in Medicine and Biology*, *52*, 6181–6196.
65. Haider, M. A., Milosevic, M., Fyles, A., Sitartchouk, I., Yeung, I., & Henderson, E. (2005). Assessment of the tumor microenvironment in cervix cancer using dynamic contrast enhanced CT, interstitial fluid pressure and oxygen measurements. *International Journal of Radiation Oncology, Biology, Physics*, *62*(4), 1100–1107.
66. Mayr, N. A., Yuh, W. T., Magnotta, V. A., Ehrhardt, J. C., Wheeler, J. A., Sorosky, J. I., et al. (1996). Tumor perfusion studies using fast magnetic resonance imaging technique in advanced cervical cancer: a new noninvasive predictive assay. *International Journal of Radiation Oncology, Biology, Physics*, *36*, 623–633.
67. Bellomi, M., Petralia, G., Sonzogni, A., Zampino, M. G., & Rocca, A. (2007). CT perfusion for the monitoring of neoadjuvant chemotherapy and radiation therapy in rectal carcinoma: initial experience. *Radiology*, *244*(2), 486–493.
68. Koukourakis, M. I., Mavanis, I., Kouklakis, G., Pitiakoudis, M., Minopoulos, G., & Manolas, C. (2007). Early antivascular effects of bevacizumab anti-VEGF monoclonal antibody on colorectal carcinomas assessed with functional CT imaging. *American Journal of Clinical Oncology*, *30*(3), 315–318.
69. Zima, A., Carlos, R., Gandhi, D., Case, I., Teknos, T., & Mukherji, S. K. (2007). Can pretreatment CT perfusion predict response of advanced squamous cell carcinoma of the upper aerodigestive tract treated with induction chemotherapy. *American Journal of Neuroradiology*, *28*(2), 328–334.
70. Makari, Y., Yasuda, T., Doki, Y., Miyata, H., Fujiwara, Y., Takiguchi, S., et al. (2007). Correlation between tumor blood Flo w assessed by perfusion CT and effect of neoadjuvant therapy in advanced esophageal Cancers. *Journal of Surgical Oncology*, *96*, 220–229.
71. Schnall, M. D., & Rosen, M. A. (2006). Primer on imaging technologies for cancer. *Journal of Clinical Oncology*, *24*(20), 3225–3233.
72. Huang, S. C. (2000). Anatomy of SUV. Standardized uptake value. *Nuclear Medicine and Biology*, *27*, 643–646.
73. Westerterp, M., Pruim, J., Oyen, W., Hoekstra, O., Paans, A., & Visser, E. (2007). Quantification of FDG PET studies using standardised uptake values in multi-centre trials: effects of image reconstruction, resolution and ROI definition parameters. *European Journal of Nuclear Medicine and Molecular Imaging*, *34*, 392–404.
74. Madsen, M. T. (2007). Recent advances in SPECT imaging. *Journal of Nuclear Medicine*, *48*(4), 661–673.
75. Beyer, T., Townsend, D. W., Brun, T., Kinahan, P. E., Charron, M., & Roddy, R. (2000). A combined PET/CT scanner for clinical oncology. *Journal of Nuclear Medicine*, *41*, 1369–1379.
76. Surti, S., Kuhn, A., Werner, M. E., Perkins, A. E., Kolthammer, J., & Karp, J. S. (2007). Performance of Philips Gemini TF PET/CT scanner with special consideration for its time-of-flight imaging capabilities. *Journal of Nuclear Medicine*, *48*, 471–480.
77. Phelps, M. E., Huang, S. C., Hoffman, E. J., & Kuhl, D. E. (1979). Validation of tomographic measurement of cerebral blood volume with C-11-labeled carboxyhemoglobin. *Journal of Nuclear Medicine*, *20*, 328–334.
78. Martin, W. R., Powers, W. J., & Raichle, M. E. (1987). Cerebral blood volume measured with inhaled C15O and positron emission tomography. *Journal of Cerebral Blood Flow and Metabolism*, *7*, 421–426.
79. Herscovitch, P., Markham, J., & Raichle, M. E. (1983). Brain blood flow measured with intravenous H2(15)O. I. Theory and error analysis. *Journal of Nuclear Medicine*, *24*, 782–789.
80. West, J. B., & Dollery, C. T. (1962). Uptake of oxygen-15-labeled CO2 compared with carbon-11-labeled CO2 in the lung. *Journal of Applied Physiology*, *17*(1), 9–13.
81. Taniguchi, H., Kunishima, S., & Koh, T. (2003). The reproducibility of independently measuring human regional hepatic arterial, portal and total hepatic blood flow using [15O]water and positron emission tomography. *Nuclear Medicine Communications*, *24*(5), 497–501.
82. Wells, P., Jones, T., & Price, P. (2003). Assessment of inter- and intrapatient variability in C15O2 positron emission tomography measurements of blood flow in patients with intra-abdominal cancers. *Clinical Cancer Research*, *9*, 6350–6356.
83. Wilson, C. B., Lammertsma, A. A., McKenzie, C. G., Sikora, K., & Jones, T. (1992). Measurements of blood flow and exchanging water space in breast tumors using positron emission tomography: a rapid and noninvasive dynamic method. *Cancer Research*, *52*, 1592–1597.
84. Mankoff, D. A., Dunnwald, L. K., Gralow, J. R., Ellis, G. K., Schubert, E. K., & Charlop, A. W. (2002). [Tc-99m]-sestamibi uptake and washout in locally advanced breast cancer are correlated with tumor blood flow. *Nuclear Medicine Biology*, *29*(7), 719–727.
85. Mankoff, D. A., Dunnwald, L. K., Gralow, J. R., Ellis, G. K., Schubert, E. K., & Tseng, J. (2003). Changes in blood flow and metabolism in locally advanced breast cancer treated with neoadjuvant chemotherapy. *Journal of Nuclear Medicine*, *44* (11), 1806–1814.
86. Miller, K. D., Soule, S. E., Calley, C., Emerson, R. E., Hutchins, G. D., & Kopecky, K. (2005). Randomized phase II trial of the anti-angiogenic potential of doxorubicin and docetaxel; primary chemotherapy as Biomarker Discovery Laboratory. *Breast Cancer Research and Treatment*, *89*(2), 187–197.
87. Kurdziel, K. A., Figg, W. D., Carrasquillo, J. A., Huebsch, S., Whatley, M., Sellers, D., et al. (2003). Using positron emission tomography 2-deoxy-2-[18F]fluoro-D-glucose, 11CO, and 15O-water for monitoring androgen independent prostate cancer. *Molecular Imaging and Biology*, *5*, 86–93.
88. Herbst, R. S., Mullani, N. A., Davis, D. W., Hess, K. R., McConkey, D. J., Charnsangavej, C., et al. (2002). Development of biologic markers of response and assessment of antiangiogenic activity in a clinical trial of human recombinant endostatin. *Journal of Clinical Oncology*, *20*(18), 3804–3814.
89. Lara, P. N., Quinn, D. I., Margolin, K., Meyers, F. J., Longmate, J., Frankel, P., et al. (2003). SU5416 plus interferon alpha in advanced renal cell carcinoma: a phase II California Cancer Consortium Study with biological and imaging correlates of angiogenesis inhibition. *Clinical Cancer Research*, *9*, 4772–4781.
90. Anderson, H., Yap, J. T., Wells, P., Miller, M. P., Propper, D. J., & Price, P. (2003a). Measurement of renal tumour and normal tissue perfusion using positron emission tomography in a phase II clinical trial of razoxane. *British Journal of Cancer*, *89*(2), 262–267.
91. Anderson, H. L., Yap, J. T., Miller, M. P., Robbins, A., Jones, T., & Price, P. M. (2003b). Assessment of pharmacodynamic vascular response in a phase I trial of combretastatin A4 phosphate. *Journal of Clinical Oncology*, *21*(15), 2823–2830.
92. Logan, T. F., Jadali, F., Egorin, M. J., Mintun, M., Sashin, D., Gooding, W. E., et al. (2002). Decreased tumor blood flow as measured by positron emission tomography in cancer patients treated with interleukin-1 and carboplatin on a phase I trial. *Cancer Chemotherapy and Pharmacology*, *50*(6), 433–444.

93. Hockel, M., Schlenger, K., Aral, B., Mitze, M., Schaffer, U., & Vaupel, P. (1996). Association between tumor hypoxia and malignant progression in advanced cancer of the uterine cervix. *Cancer Research*, *56*(19), 4509–4515.
94. Fyles, A., Milosevic, M., Hedley, D., Pintilie, M., Levin, W., & Manchul, L. (2002). Tumor hypoxia has independent predictor impact only in patients with nodenegative cervix cancer. *Journal of Clinical Oncology*, *20*(3), 680–687.
95. Brizel, D. M., Dodge, R. K., Clough, R. W., & Dewhirst, M. W. (1999). Oxygenation of head and neck cancer: changes during radiotherapy and impact on treatment outcome. *Radiotherapy and Oncology*, *53*, 113–117.
96. Brizel, D. M., Scully, S. P., Harrelson, J. M., Layfield, L. J., Bean, J. M., & Prosnitz, L. R. (1996). Tumor oxygenation predicts for the likelihood of distant metastases in human soft tissue sarcoma. *Cancer Research*, *56*, 941–943.
97. Nordsmark, M., Alsner, J., Keller, J., Nielsen, O. S., Jensen, O. M., & Horsman, M. R. (2001). Hypoxia in human soft tissue sarcomas: adverse impact on survival and no association with p53 mutations. *British Journal of Cancer*, *84*(8), 1070–1075.
98. Nordsmark, M., & Overgaard, J. (2000). A confirmatory prognostic study on oxygenation status and loco-regional control in advanced head and neck squamous cell carcinoma treated by radiation therapy. *Radiotherapy and Oncology: Journal of the European Society for Therapeutic Radiology and Oncology*, *57*, 39–43.
99. Rudat, V., Vanselow, B., Wollensack, P., Bettscheider, C., Osman-Ahmet, S., & Eble, M. J. (2000). Repeatability and prognostic impact of the pretreatment pO(2) histography in patients with advanced head and neck cancer. *Radiotherapy and Oncology: Journal of the European Society for Therapeutic Radiology and Oncology*, *57*, 31–37.
100. Padhani, A. R., Krohn, K. A., Lewis, J. S., & Alber, M. (2007). Imaging oxygenation of human tumours. *European Radiology*, *17*, 861–872.
101. Rischin, D., Hicks, R. J., Fisher, R., Binns, D., Corry, J., & Porceddu, S. (2006). Prognostic significance of [18F]-misonidazole positron emission tomography-detected tumor hypoxia in patients with advanced head and neck cancer randomly assigned to chemoradiation with or without tirapazamine: a substudy of Trans-Tasman Radiation Oncology Group Study 98.02. *Journal of Clinical Oncology*, *24*, 2098–2104.
102. Gagel, B., Reinartz, P., Demirel, C., Kaiser, H. J., Zimny, M., Piroth, M., et al. (2006). [18F] fluoromisonidazole and [18F] fluorodeoxyglucose positron emission tomography in response evaluation after chemo-/radiotherapy of non-small-cell lung cancer: a feasibility study. *BMC Cancer*, *6*, 51.
103. Cher, L. M., Murone, C., Lawrentschuk, N., Ramdave, S., Papenfuss, A., Hannah, A., et al. (2006). Correlation of hypoxic cell fraction and angiogenesis with glucose metabolic rate in gliomas using 18Ffluoromisonidazole, 18F-FDG PET, and immunohistochemical studies. *Journal of Nuclear Medicine*, *47*, 410–418.
104. Bruehlmeier, M., Roelcke, U., Schubiger, P. A., & Ametamey, S. M. (2004). Assessment of hypoxia and perfusion in human brain tumors using PET with 18F-fluoromisonidazole and 15O-H2O. *Journal of Nuclear Medicine*, *45*, 1851–1859.
105. Swietach, P., Vaughan-Jones, R. D., & Harris, A. L. (2007). Regulation of tumor pH and the role of carbonic anhydrase 9. *Cancer and Metastasis Reviews*, *26*, 299–310.
106. Steffens, M. G., Boerman, O. C., Oosterwijk-Wakka, J. C., Oosterhof, G. O., Witjes, J. A., Koenders, E. B., et al. (1997). Targeting of renal cell carcinoma with iodine-131-labeled chimeric monoclonal antibody G250. *Journal of Clinical Oncology*, *15*, 1529–1537.
107. Brouwers, A. H., Buijs, W. C., Oosterwijk, E., Boerman, O. C., Mala, C., & De Mulder, P. H. (2003). Targeting of metastatic renal cell carcinoma with the chimeric monoclonal antibody G250 labeled with (131)I or (111)In: an intrapatient comparison. *Clinical Cancer Research*, *9*, 3953S–3960S.
108. Steffens, M. G., Oosterwijk, E., Kranenborg, M. H., Manders, J. M., Debruyne, F. M., & Corstens, F. H. (1999). *In vivo* and *in vitro* characterizations of three 99mTc-labeled monoclonal antibody G250 preparations. *Journal of Nuclear Medicine*, *40*, 829–836.
109. Divgi, C. R., O'Donoghue, J. A., Welt, S., O'Neel, J., Finn, R., Motzer, R. J., et al. (2004). Phase I clinical trial with fractionated radioimmunotherapy using 131I-labeled chimeric G250 in metastatic renal cancer. *Journal of Nuclear Medicine*, *45*, 1412–1421.
110. Divgi, C. R., Pandit-Taskar, N., Jungbluth, A. A., Reuter, V. E., Gönen, M., Ruan, S., et al. (2007). Preoperative characterization of clear-cell renal carcinoma using iodine-124-labelled antibody chimeric G250 (124IcG250) and PET in patients with renal masses: a phase I trial. *Lancet Oncology*, *8*, 304–310.
111. Warburg, O. (1956). On the origin of cancer cells. *Science*, *123* (3191), 309–314.
112. Bos, R., van Der Hoeven, J. J., van Der Wall, E., van Der Groep, P., van Diest, P. J., Comans, E., et al. (2002). Biologic correlates of (18) fluorodeoxyglucose uptake in human breast cancer measured by positron emission tomography. *Journal of Clinical Oncology*, *20* (2), 379–387.
113. Zasadny, K. R., Tatsumi, M., & Wahl, R. L. (2003). FDG metabolism and uptake versus blood flow in women with untreated primary breast cancers. *European Journal of Nuclear Medicine Molecular Imaging*, *30*(2), 274–280.
114. Li, K., Wilmes, L. J., Henry, R. G., Pallavicini, M. G., Park, J. W., Hu-Lowe, D. D., et al. (2005). Heterogeneity in the angiogenic response of a BT474 human breast cancer to a novel vascular endothelial growth factor-receptor tyrosine kinase inhibitor: assessment by voxel analysis of dynamic contrast-enhanced MRI. *Journal of Magnetic Resonance Imaging*, *22*, 511–519.
115. Jayson, G. C., Zweit, J., Jackson, A., Mulatero, C., Julyan, P. J., Ranson, M., et al. (2002). Molecular imaging and biological evaluation of HuMV833 anti-VEGF antibody: implications for trial design of antiangiogenic antibodies. *Journal of the National Cancer Institute*, *24*(19), 1484–1493.
116. Cai, W., Chen, K., Mohamedali, K. A., Cao, Q., Gambhir, S. S., & Rosenblum, M. G. (2006). PET of vascular endothelial growth factor receptor expression. *Journal of Nuclear Medicine*, *47*(12), 2048–2056.
117. Hsu, A. R., Cai, W., Veeravagu, A., Mohamedali, K. A., Chen, K., Kim, S., et al. (2007). Multimodality molecular imaging of glioblastoma growth inhibition with vasculature-targeting fusion toxin VEGF121/rGel. *Journal of Nuclear Medicine*, *48*(3), 445–454.
118. Collingridge, D. R., Carroll, V. A., Glaser, M., Aboagye, E. O., Osman, S., Hutchinson, O. C., et al. (2002). The development of [(124)I]iodinated-VG76e: a novel tracer for imaging vascular endothelial growth factor *in vivo* using positron emission tomography. *Cancer Research*, *62*, 5912–5919.
119. Sivolapenko, G. B., Skarlos, D., Pectasides, D., Stathopoulou, E., Milonakis, A., & Sirmalis, G. (1998). Imaging of metastatic melanoma utilising a technetium-99m labelled RGD-containing synthetic peptide. *European Journal of Nuclear Medicine*, *25*(10), 1383–1389.
120. Haubner, R., Wester, H. J., Weber, W. A., Mang, C., Ziegler, S. I., & Goodman, S. L. (2001). Noninvasive imaging of alpha(v)beta3 integrin expression using 18F-labeled RGD-containing glycopeptide and positron emission tomography. *Cancer Research*, *61*, 1781–1785.
121. Beer, A. J., Haubner, R., Sarbia, M., Goebel, M., Luderschmidt, S., Grosu, A. L., et al. (2006). Positron emission tomography using

[18F]Galacto-RGD identifies the level of integrin alpha(v)beta3 expression in man. *Clinical Cancer Research*, *12*(13), 3942–3949.
122. Chen, X., Park, R., Khankaldyyan, V., Gonzales-Gomez, I., Tohme, M., & Moats, R. A. (2006). Longitudinal microPET imaging of brain tumor growth with F-18-labeled RGD peptide. *Molecular Imaging and Biology*, *8*(1), 9–15.
123. Jung, K. H., Lee, K. H., Paik, J. Y., Ko, B. H., Bae, J. S., & Lee, B. C. (2006). Favorable biokinetic and tumor-targeting properties of 99mTc-labeled glucosamino RGD and effect of paclitaxel therapy. *Journal of Nuclear Medicine*, *47*(12), 2000–2007.
124. Meyerowitz, C. B., Fleischer, A. C., Pickens, D. R., Thurman, G. B., Borowsky, A. D., & Thirsk, G. (1996). Quantification of tumor vascularity and flow with amplitude color Doppler sonography in an experimental model: preliminary results. [erratum appears in J Ultrasound Med 1997 Mar;16(3):218]. *Journal of Ultrasound Medicine*, *15*, 827–833.
125. Arger, P. H., Malkowicz, S. B., VanArsdalen, K. N., Sehgal, C. M., Holzer, A., & Schultz, S. M. (2004). Color and power Doppler sonography in the diagnosis of prostate cancer: comparison between vascular density and total vascularity. *Journal of Ultrasound in Medicine*, *23*, 623–630.
126. Yang, W. T., Tse, G. M. K., Lam, P. K. W., Metreweli, C., & Chang, J. (2002). Correlation between color power Doppler sonographic measurement of breast tumor vasculature and immunohistochemical analysis of microvessel density for the quantitation of angiogenesis. *Journal Ultrasound in Medicine*, *21*, 1227–1235.
127. Ferrara, K. W., Merritt, C. R., Burns, P. N., Foster, F. S., Mattrey, R. F., & Wickline, S. A. (2000). Evaluation of tumor angiogenesis with US: imaging, Doppler, and contrast agents. *Academic Radiology*, *7*, 824–839.
128. Sehgal, C. M., Arger, P. H., Rowling, S. E., Conant, E. F., Reynolds, C., & Patton, J. A. (2000). Quantitative vascularity of breast masses by Doppler imaging: regional variations and diagnostic implications. *Journal of Ultrasound Medicine*, *19*, 427–440 quiz 441–422.
129. Wood, A. K. W., Ansaloni, S., Ziemer, L. S., Lee, W. M. F., Feldman, M. D., & Sehgal, C. M. (2005). The antivascular action of physiotherapy ultrasound on murine tumors. *Ultrasound in Medicine Biology*, *31*, 1403–1410.
130. Kamotani, Y., Lee, W. M. F., Arger, P. H., Cary, T. W., & Sehgal, C. M. (2003). Multigated contrast-enhanced power Doppler to measure blood flow in mice tumors. *Ultrasound in Medicine Biology*, *29*, 977–984.
131. Bertolotto, M., Pozzato, G., Croce, L. S., Nascimben, F., Gasparini, C., & Cova, M. A. (2006). Blood flow changes in hepatocellular carcinoma after the administration of thalidomide assessed by reperfusion kinetics during microbubble infusion: preliminary results. *Investigative Radiology*, *41*, 15–21.
132. McCarville, M. B., Streck, C. J., Dickson, P. V., Li, C.-S., Nathwani, A. C., & Davidoff, A. M. (2006). Angiogenesis inhibitors in a murine neuroblastoma model: quantitative assessment of intratumoral blood flow with contrast-enhanced gray-scale US.[see comment]. *Radiology*, *240*, 73–81.
133. Thomas, J. P., Arzoomanian, R. Z., Alberti, D., Marnocha, R., Lee, F., Friedl, A., et al. (2003). Phase I pharmacokinetic and pharmacodynamic study of recombinant human endostatin in patients with advanced solid tumors. *Journal of Clinical Oncology*, *21*, 223–231.
134. Hsu, C., Chen, C. N., Chen, L. T., Wu, C. Y., Hsieh, F. J., & Cheng, A. L. (2005). Effect of thalidomide in hepatocellular carcinoma: assessment with power Doppler US and analysis of circulating angiogenic factors. *Radiology*, *235*, 509–516.
135. Yodh, A. G., & Chance, B. (1995). Spectroscopy and imaging with diffusing light. *Physics Today*, *48*, 34–40.
136. Yodh, A. G., & Boas, D. (2003). Functional imaging with diffusing light. *Biomedical Photonics Handbook*, *21*(1), 21–45.
137. Intes, X., Ripoll, J., Chen, Y., Nioka, S., Yodh, A. G., & Chance, B. (2003). *In vivo* continuous-wave optical breast imaging enhanced with Indocyanine Green. *Medical Physics*, *30*, 1039–1047.
138. Ntziachristos, V., Yodh, A. G., Schnall, M. D., & Chance, B. (2000). Concurrent MRI and diffuse optical tomography of breast after indocyanine green enhancement. *Proceedings of the National Academy of Sciences of the United States of America*, *97*(6), 2767–2772.
139. Corlu, A., Choe, R., Durduran, T., Rosen, M. A., Schweiger, M., & Arridge, S. R. (2007). Three-dimensional *in vivo* fluorescence diffuse optical tomography of breast cancer in humans. *Optics Express*, *15*(11), 1–21.
140. Jakubowski, D. B., Cerussi, A. E., Bevilacqua, F., Shah, N., Hsiang, D., & Butler, J. (2004). Monitoring neoadjuvant chemotherapy in breast cancer using quantitative diffuse optical spectroscopy: a case study. *Journal of Biomedical Optics*, *9*(1), 230–238.
141. Choe, R., Corlu, A., Lee, K., Durduran, T., Konecky, S. D., Grosicka-Koptyra, M., et al. (2005). Diffuse optical tomography of breast cancer during neoadjuvant chemotherapy: a case study with comparison to MRI. *Medical Physics*, *32*(4), 1128–1139.
142. Zhu, Q., Kurtzma, S. H., Hegde, P., Tannenbaum, S., Kane, M., Huang, M., et al. (2005). Utilizing optical tomography with ultrasound localization to image heterogeneous hemoglobin distribution in large breast cancers. *Neoplasia*, *7*(3), 263–270.
143. Cerussi, A. E., Hsiang, D., Shah, N., Mehta, R., Durkin, A., & Butler, J. (2007). Predicting response to breast cancer neoadjuvant chemotherapy using diffuse optical spectroscopy. *Proceeding of the National Academy Science USA*, *104*(10), 4014–4019.
144. Zhou, C., Choe, R., Shah, N., Durduran, T., Yu, G., Durkin, A., et al. (2007). Diffuse optical monitoring of blood flow and oxygenation in human breast cancer during early stages of neoadjuvant chemotherapy. *Journal of Biomedical Optics*, *12*, 051903.
145. Sunar, U., Quon, H., Durduran, T., Zhang, J., Du, J., Zhou, C., et al. (2006). Noninvasive diffuse optical measurement of blood flow and blood oxygenation for monitoring radiation therapy in patients with head and neck tumors: a pilot study. *Journal of Biomedical Optics*, *11*(6), 064021.
146. Yu, G., Durduran, T., Zhou, C., Zhu, T. C., Finlay, J. C., & Busch, T. M. (2006). Real-time in situ monitoring of human prostate photodynamic therapy with diffuse light. *Photochemistry and Photobiology*, *82*(5), 1279–1284.
147. Sunar, U., Makonnen, S., Zhou, C., Durduran, T., Yu, G., Wang, H., et al. (2007). Hemodynamic responses to antivascular therapy and ionizing radiation assessed by diffuse optical spectroscopies. *Optics Express*, *15*, 15507–15516.